VOL. 10, NO. 19, OCTOBER 2015 ISSN 1819-6608
ARPN Journal of Engineering and Applied Sciences

www.arpnjournals.com

SLOTTED ULTRA WIDEBAND (UWB) ANTENNA WITH ENHANCED BANDWIDTH FOR WIRELESS APPLICATIONS

Lee Chia Ping
School of Engineering, Taylor's University Lakeside Campus, No.1, Jalan Taylor's, Subang Jaya, Selangor, Malaysia
E-Mail: ChiaPing.Lee@taylors.edu.my

ABSTRACT

Slotted Ultra Wideband (UWB) microstrip patch antenna with enhanced bandwidth is presented in this paper. The proposed antenna is simulated in CST Microwave Studio and fabricated for measurements. Its simulated result displays impedance bandwidth with S_{11} below -15 dB from 3.3 GHz to 19.53 GHz, whereas the measured result displays the operating frequency region from 3 GHz to 18.6 GHz. The antenna exhibits excellent UWB characteristics with the return loss of S_{11}<-10 dB and Voltage Standing Wave Ratio (VSWR) ≤ 2 throughout the impedance bandwidth. Besides, the antenna also displays good linearity and stable radiation patterns. This antenna has successfully exceeded the bandwidth of UWB requirement, which is from 3.1 GHz to 10.6 GHz, and can be suited easily with portable devices in wireless applications.

Keywords: ultra wideband, antenna, bandwidth, return loss, radiation pattern.

INTRODUCTION

Ultra Wideband (UWB) has been described as the emerging technology, following the release of its extremely wide spectrum, which is from 3.1 GHz to 10.6 GHz. Following such mandate by the Federal Communications Commission (FCC, 2002), researches on development of UWB antenna have gained tremendous interest by both academia and industries. Since the power spectral mask of UWB signal assigned by FCC is to not exceed -41.3 dBm/MHz, it allows the UWB devices to overlay existing communication systems while ensuring successful control of interference.

The bandwidth of the fundamental resonant frequency and other harmonic frequencies of an antenna are mainly determined by its shape, structure, size, material and feed system. For instance, helical-beam antenna, biconical antenna, spiral antenna and log-periodic antenna are among the types and structures used to obtain the required bandwidth. The drawback on these antennas includes the difficulty to be used especially in the mobile system due to their size and narrow radiation pattern.

Researches on antennas are driven by several factors. Most importantly, the minimization size of the antenna is the main focus, so as to be made compatible with portable devices (Guo *et al.* 2007). This reasons well with keeping the cost production to the minimum, as well as replacing the other bulky antenna structures as mentioned earlier. Therefore, microstrip patch antennas are in favour for antenna design due to its features of being low profile, light weight, small size and compact (Zehforoosh *et al.* 2007).

However, the main challenge in designing a UWB antenna is the narrowband characteristic of the microstrip patch antenna itself. Numerous researches have been done mainly to increase the impedance bandwidth, one of which includes the study of ordinary slot antenna with S-shaped slots (Ojaroudi *et al.* 2013). The study achieved 130% of fractional bandwidth but at the expense of band-notched function from 5 GHz to 6 GHz. Addaci *et al.* designed a monopole antenna with modified ground plane and loop feeding structure on PCB, which observed relative bandwidth of 110% (Addaci *et al.* 2014). Guo *et al.* included electromagnetic bandgap structure as the bandwidth enhancement technique (Guo *et al.* 2013). Fractal geometry designs were utilized by Tripathi *et al.* and Tsai, achieving 3 GHz to 12.8 GHz (Tripathi *et al.* 2014) and 1.85 GHz to 6.3 GHz (Tsai, 2014), respectively. Falahati *et al.* utilized the Penta-Gasket-Koch design on monopole antenna using co-planar waveguides to operate from 5.35 GHz to 7.35 GHz and 10.07 GHz to 11 GHz (Falahati *et al.* 2011). M. Islam *et al.* presented a negative index metamaterial incorporated UWB antenna to enhance its sensor performance with bandwidth of 131.5% (Islam *et al.* 2015).

This paper proposes an edge-fed microstrip slotted patch antenna which achieves the UWB bandwidth enhancement, as the antenna functions with the impedance bandwidth from 3.3 GHz to 19.53 GHz. Next section describes the antenna design, in which basic configuration of the antenna is explained. This is followed by detailed discussion of the antenna performance in terms of its return loss, phase angle, voltage standing wave ratio and radiation patterns. Lastly, the conclusion highlights the summary of the findings of the antenna. Overall, the proposed antenna exhibits a fractional bandwidth of 142.18% for its simulated result, while the measured result displays 144.44%. The simple bandwidth enhancement technique by modifying the antenna parameters does perform better result in terms of the attainment of enhanced bandwith, with total bandwidth of 16.32 GHz, compared to prong-shaped and rake-shaped antenna of 7.5 GHz (Fayadh *et al.* 2014), tapered step co-planar waveguide fed antenna of 13 GHz (Madhav *et al.* 2014) and L and W-shaped slotted antenna with operating bandwidth of 15.73 GHz (Raj *et al.* 2014). It is noted that the proposed antenna achieves 117.6% bandwidth as compared to rake-shaped antenna of similar size (Fayadh *et al.* 2014) and a reduction of 64% in terms of its antenna

VOL. 10, NO. 19, OCTOBER 2015 ISSN 1819-6608
ARPN Journal of Engineering and Applied Sciences

www.arpnjournals.com

size compared to (Tsai, 2014). A small compact antenna with improved performance is crucial as it keeps its fabrication cost to its minimum.

ANTENNA DESIGN

Basic configuration

The antenna design is depicted in Figure-1, comprising both front and back part of the antenna. The antenna is designed on a double-sided FR4 substrate with the thickness of 1.6 mm and dielectric constant of 3.8.

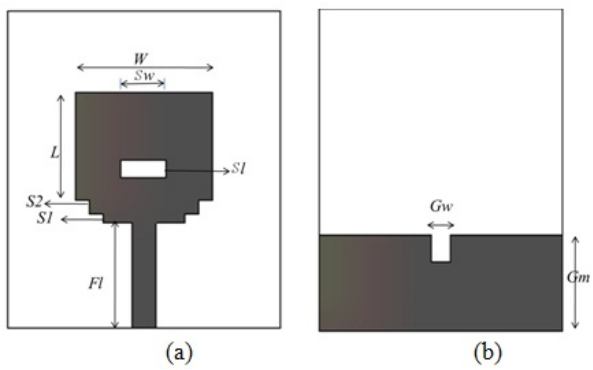

Figure-1. Basic configuration of (a) Patch antenna (b) Ground plane.

The front part of the antenna consists of a larger patch with a square slot and a smaller patch which serves as the feedline, as illustrated in Figure 1a. The patch antenna's width and length are denoted by '*W*' and '*L*' respectively. The bottom part of the patch antenna is modified into steps denoted by '*S1*' and '*S2*'. Meanwhile, the dimension of the rectangular slot is represented by '*Sl*' and '*Sw*'. The feedline is denoted by '*Fl*'. The patch antenna structure is printed on one side of the FR4 substrate with the ground on the other side. The back part of the antenna consists of a partial ground plane, as illustrated in Figure 1b. The ground plane is denoted by '*Gw*' and '*Gm*'. The design parameters such as the patch shape, step, the feedline width and notched partial ground plane are optimized to obtain the best return loss, S_{11} and impedance bandwidth before determining the best dimensions for the proposed antenna. All the simulations are carried out using CST Microwave Studio. The fabricated antenna is as illustrated in Figure-2.

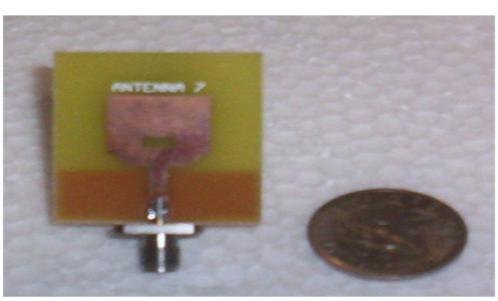

Figure-2. Fabricated antenna.

The dimensions of the antenna structure are as shown in Table-1.

Table-1. Dimension of the antenna design.

Basic configuration	Variable	Dimension (mm)
Patch antenna	*W*	15.0
	L	14.5
	S1	1.0
	S2	1.5
	Fl	11.5
Slot	*Sl*	2.0
	Sw	5.0
Ground plane	*Gw*	2.7
	Gm	10.5

RESULTS AND DISCUSSIONS

Return loss

Figure-3 illustrates the simulated and measured return loss of the proposed antenna against the frequency. Based on the simulated results, the antenna displays resonant frequencies 4.64 GHz with S_{11} of -22.13 dB, 6.41 GHz with S_{11} of -23.46 dB, 10.48 GHz with S_{11} of -29.94 dB, 15.5 GHz with S_{11} of -19.73 dB and 18.1 GHz with S_{11} of -16.02 dB.

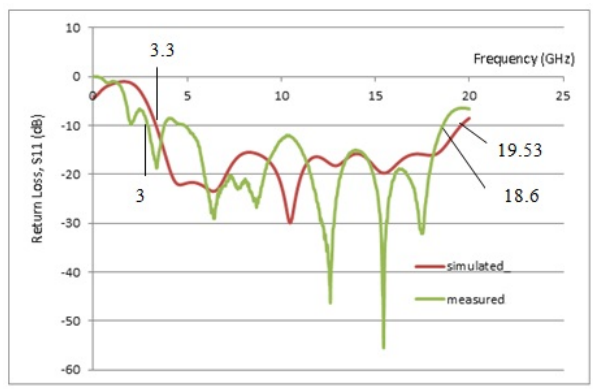

Figure-3. Return loss, S_{11} (dB) against frequency (GHz).

The resonant frequency at 4.64 GHz is due to the patch length, '*L*'. The patch length is resonant at TEM_{010} mode, which can be validated in equation (1), given by (Balanis, 2005).

$$f_{res,mnp} = \frac{1}{2\pi\sqrt{\mu\varepsilon}}\sqrt{\left(\frac{m\pi}{W}\right)^2 + \left(\frac{n\pi}{L}\right)^2 + \left(\frac{p\pi}{h}\right)^2} \quad (1)$$

f = resonant frequency,
W = width of patch antenna,
L = length of patch antenna

Based on the lowest resonant frequency, the effective current path length '*L*' from the patch is calculated to be 0.7λ by using the equations (2) and (3) (Chen, 2007).

$$f = \frac{c}{\lambda} \quad (2)$$

f = resonant frequency,
λ = wavelength at f
c = velocity of light

$$\lambda = 2L\sqrt{(\varepsilon_r + 1)/2} \quad (3)$$

ε_r = relative permittivity
L = length of patc h antenna

The rectangular slot of the patch antenna takes place in the active zone, which controls the impedance bandwidth (Pele, 2004) by introducing a capacitive reactance to counteract with the inductive reactance of the feed. The length of the slot is calculated to be approximately half-wavelength (0.5λ) at its resonant frequency at 12.8 GHz. The simulated result displays an impedance bandwidth with S_{11} below -15 dB from 3.3 GHz to 19.53 GHz, equivalent to 142.18% of fractional bandwidth. The steps at the bottom of the patch antenna tune the capacitive coupling between the patch antenna and the ground plane and thus, modify the electric and magnetic field distributions near the discontinuity of antenna geometry.

The measured result displays similar pattern as of the simulated result, except with sharper curves or lower return loss values. The impedance bandwidth of the measured result covers the range from 3 GHz to 18.6 GHz. The difference of the graphs could be due to the etching problem encountered during the antenna fabrication. A tiny misalignment of the antenna design mask on the substrate, during the fabrication, could affect the return loss of the antennas. Besides, the difference could also be due to the loss suffered in the SMA connector and the oxidation of the copper layer of the patch antenna to the air over the time. Overall, the measured antenna records a fractional bandwidth of 144.44%. The antenna performance adheres very well with the UWB characteristic, while displaying good bandwidth enhancement. In fact, the proposed antenna possesses a larger impedance bandwidth compared to the literatures mentioned earlier, such as Addaci *et al.* with 110% fractional bandwidth, Tripathi *et al.* with impedance bandwidth from 3 GHz to 12.8 GHz and Tsai (1.85 GHz to 6.3 GHz).

Phase angle

Figure-4 illustrates the simulated and measured phase angle against frequency of the antenna. Based on the simulated result, it is observed that Figure-3 shows a linear response throughout the frequency region except the range from 7.58 GHz to 13.92 GHz, in which the pulse components in this range are radiated without distortion. As for the measured result, the frequency region displays linear response until 10.52 GHz. The discrepancy in the linearity could be due to the mismatching of the input impedance for one or several frequencies. Overall, the phase angel pattern for this antenna is satisfactory.

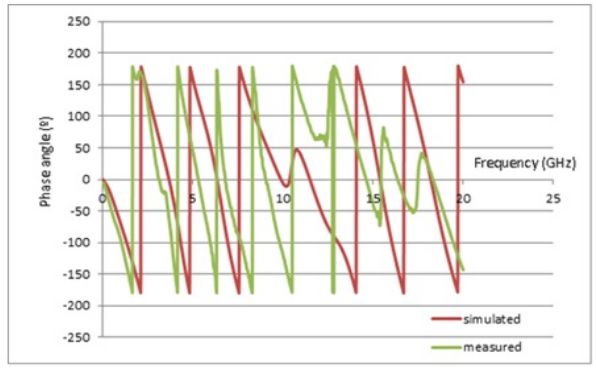

Figure-4. Phase angle (º) against frequency (GHz).

Voltage standing wave ratio (VSWR)

Figure-5 illustrates the simulated and measured voltage standing wave ratio (VSWR) against frequency of the antenna.

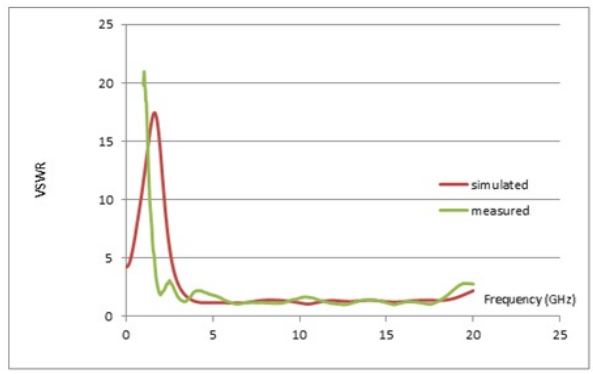

Figure-5. Voltage standing wave ratio (VSWR) against frequency (GHz).

Based on the simulated result, the VSWR value ranges from 1 to 2 throughout the operating frequency from 3.3 GHz to 19.53 GHz, which fulfills the UWB characteristic. Meanwhile, the measured result displays VSWR values from 1 to 2 except for frequency region from approximately 4.13 GHz to 4.41 GHz and 18.28 GHz to 20 GHz. Both results are validated because the same frequency regions do fall in S_{11} below -10 dB as is shown in Figure 3. This is due to the fact that return loss below -9.5 dB is indicated by VSWR from 1 to 2.

Radiation patterns

Figure-6 illustrates the simulated radiation patterns at different frequencies from 3 GHz to 9 GHz at theta cut of 90º, which is the *E*-plane. The radiation patterns are simulated with the increasing frequency step of 2 GHz.

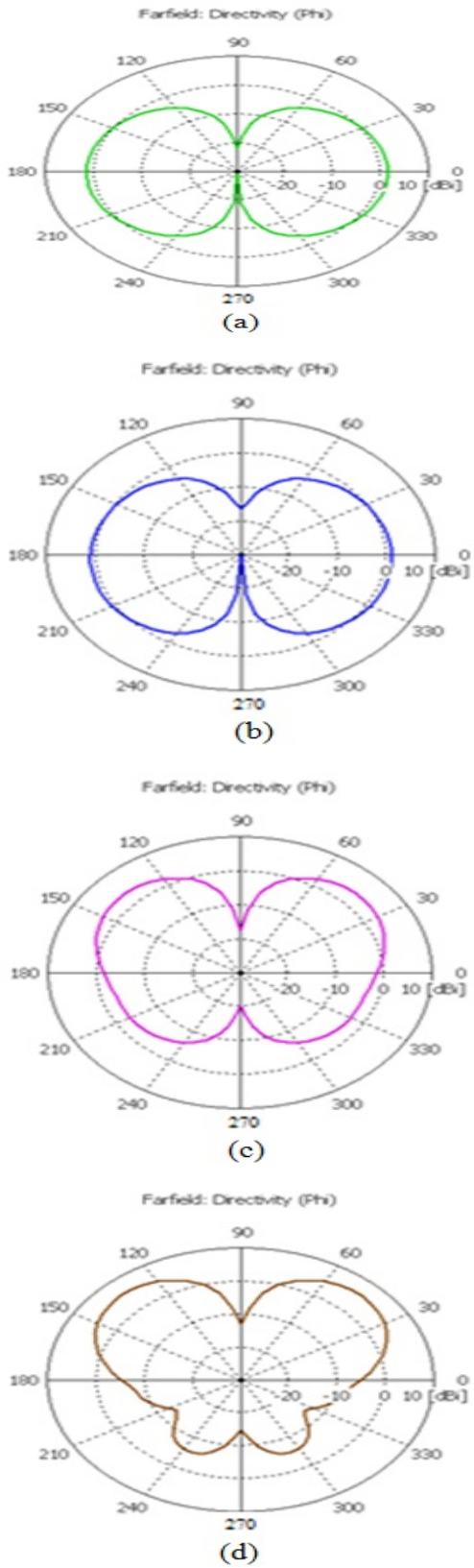

Figure-6. Radiation patterns at theta cut of 90º at (a) 3 GHz, (b) 5 GHz, (c) 7 GHz and (d) 9 GHz.

Based on Figure-6a, it is observed that the radiation patterns display a directional behavior, with its main lobe direction at 0º and 180º. This indicates that the concentration of the field focuses on the sides of the patch. Meanwhile, the lobes are suppressed at 90º and 270º, which originate from the front part and back part of the patch antenna respectively. Figure-6b and 6c exhibit a similar pattern as Figure-6a, while Figure-6d exhibits the main lobe direction at the front patch antenna from 0º to 180º. It is observed that the directivity of the antenna increases with increasing frequency, as the concentration of the field gradually focuses on the front part of the patch antenna as is observed from Figure-6. It is also obvious that more lobes are observed at the higher frequency of 9 GHz.

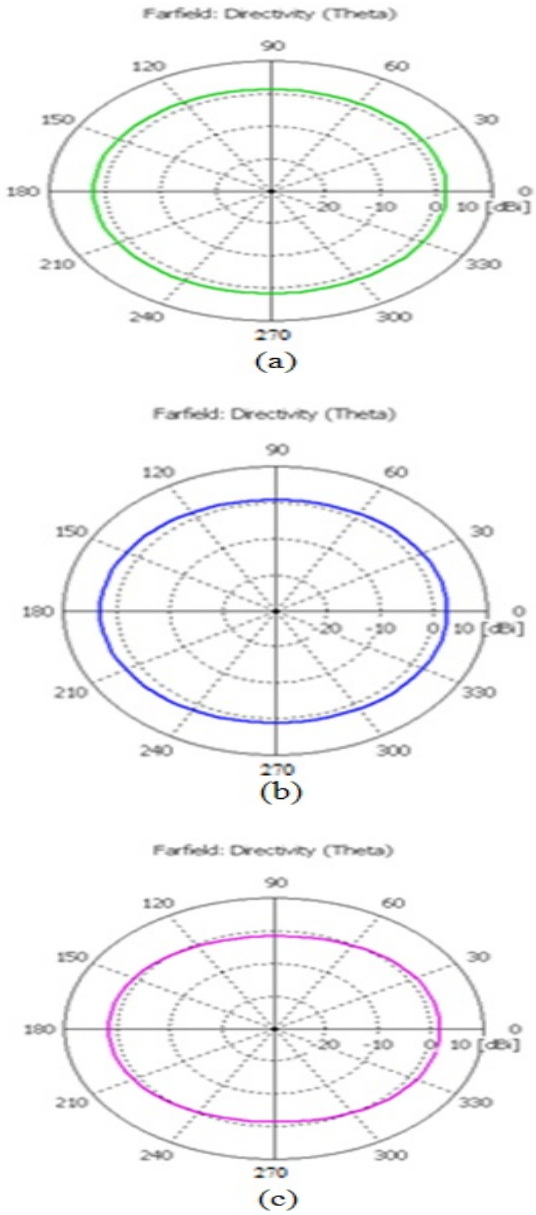

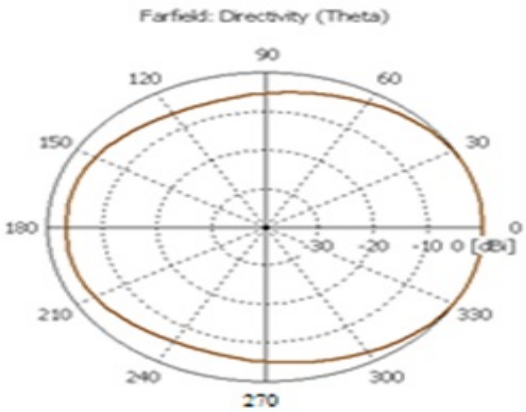

(d)

Figure-7. Radiation Patterns at Phi Cut of 0º at (a) 3 GHz, (b) 5 GHz, (c) 7 GHz and (d) 9 GHz.

Meanwhile, Figure-7 illustrates the simulated radiation patterns at different frequencies from 3 GHz to 9 GHz at phi cut of 90º, which is the *H*-plane. The radiation patterns are simulated with the increasing frequency step of 2 GHz. Based on Figure 7, it is observed that the radiation patterns exhibit an omnidirectional behavior, which indicates that the concentration of the fields distribute evenly across the *H*-plane of the antenna.

CONCLUSIONS

The paper proposes an antenna which exhibits excellent UWB characteristics, with its simulated result displaying an impedance bandwidth with S_{11} below -15 dB from 3.3 GHz to 19.53 GHz. This is equivalent to 142.18% of fractional bandwidth. The theoretical result of the antenna is validated by the measured result which displays similar result with the impedance bandwidth from from 3 GHz to 18.6 GHz, totaling to fractional bandwidth of 144.44%. The slight difference in both simulated and measured result could be due to the fabrication tolerances. The proposed antenna also has successfully achieved enhanced UWB bandwidth, in which UWB frequency spectrum covers the range from 3.1 GHz to 10.6 GHz. It also complies very well with the VSWR below 2 throughout the operating frequency region. The antenna is analyzed of its linearity through the phase angle. Radiation patterns of the antenna observe an increasing directivy of the antenna with increasing frequency on *E*-plane. Meanwhile, the radiation patterns are observed to be omnidirectional on *H*-plane, indicating a well-distributed field concentration of the antenna. The proposed antenna exhibits excellent UWB characteristics and suits very well with the portable devices for wireless applications.

REFERENCES

[1] Addaci R., Hamdiken N., Fortaki T., Ferrero F., Seetharamdoo D. and Staraj R. 2014. Simple Bandwidth-Enhancement Technique for Miniaturised Low-Profile UWB Antenna Design. ELECTRON LETT, Electronics Letters, Vol. 50, No. 22, pp. 1564-1566.

[2] Balanis C. A. 2005. Antenna Theory Analysis and Design. 3rd Ed. N.J: John Wiley and Sons.

[3] Chen Z. N. 2007. Antenna for Portable Device. England: John Wiley & Sons.

[4] Falahati a., Naghshvarian-Jahromi M. and Edwards R.M. 2011. Bandwidth enhancement and decreasing ultra-wideband pulse response distortion of Penta–Gasket–Koch monopole antennas using compact-grounded co-planar wave guides. IET Microwaves, Antennas & Propagation, Vol. 5, No. 1, p.48.

[5] Fayadh R. A., Malek F., Fadhil H. A. and Aldhaibani J.A. 2014. The performance of two antenna design shapes in ultra-wideband wireless applications. , ARPN Journal of Engineering and Applied Sciences, Vol. 9, No. 1, pp.12–19.

[6] FCC 2002. First report and order 02-48 (FCC 02-48).

[7] Guo L., Wang S., Chiau C.C., Chen X. and Parini C.G. 2007. On small UWB antennas. EuCAP 2007,The Second European Conference on Antennas and Propagation, pp. 1-6.

[8] Islam M. *et al.* 2015. A Negative Index Metamaterial-Inspired UWB Antenna with an Integration of Complementary SRR and CLS Unit Cells for Microwave Imaging Sensor Applications. Sensors, Vol. 15, No. 5, pp.11601–11627.

[9] Ojaroudi N. and Ojaroudi M. 2013. Bandwidth Enhancement of an Ultra-Wideband Printed Slot Antenna with WLAN Band-Notched Function. Microwave and Optical Technology Letters, Vol. 55, No. 7, pp. 1448–1451.

[10] Madhav B. T. P., Kotamraju F. K., Manikanta P., Narendra K., Kishore M. R. and Kiran G. 2014. Tapered step cpw-fed antenna for wideband applications. , ARPN Journal of Engineering and Applied Sciences, Vol. 9, No. 10, pp.1967–1973.

[11] Pele I. 2004. Antenna Design with Control of Radiation Pattern and Frequency Bandwidth. IEEE Antennas and Propagation Society International Symposium, pp. 783 – 786.

[12] Raj R. K., Singh A., Rathore K., Buldak M. and Sharma R. 2014. An UWB Dual Band Notched Antenna with W-slot and Enhanced Bandwidth. 2014 International Conference on Medical Imaging, m-Health and Emerging Communication Systems (MedCom), 7-8 Nov., pp. 126 – 130, Greater Noida.

[13] Tripathi S., Yadav S. and Mohan A. 2014. Hexagonal fractal ultra-wideband antenna using Koch geometry with bandwidth enhancement. IET Microwaves, Antennas & Propagation, Vol. 8, No. 15, pp.1445–1450.

[14] Tsai L. 2014 Bandwidth Enhancement in Coplanar Waveguide-Fed Slot Antennas Designed For Wideband Code Division Multiple Access/Wireless Local Area Network/ Worldwide Interoperability for Microwave Access Applications. IET Microwaves, Antennas & Propagation, Vol. 8, No. 10, pp. 724-729.

[15] Zehforoosh Y., Ghobadi C. and Nourinia J. 2007 Antenna design for Ultra Wideband application using a new multilayer structure. PIERS 2007, Progress In Electromagnetics Research Symposium 2007, pp. 544-549.